

Accepted Manuscript

A facile strategy toward 3D hydrophobic composite resin network decorated with biological ellipsoidal structure rapeseed flower carbon for enhanced oils and organic solvents selective absorption

Jian Rong, Fengxian Qiu, Tao Zhang, Xiaoying Zhang, Yao Zhu, Jicheng Xu, Dongya Yang, Yuting Dai

PII: S1385-8947(17)30586-7
DOI: <http://dx.doi.org/10.1016/j.cej.2017.04.049>
Reference: CEJ 16803

To appear in: *Chemical Engineering Journal*

Received Date: 24 January 2017
Revised Date: 21 March 2017
Accepted Date: 11 April 2017

Please cite this article as: J. Rong, F. Qiu, T. Zhang, X. Zhang, Y. Zhu, J. Xu, D. Yang, Y. Dai, A facile strategy toward 3D hydrophobic composite resin network decorated with biological ellipsoidal structure rapeseed flower carbon for enhanced oils and organic solvents selective absorption, *Chemical Engineering Journal* (2017), doi: <http://dx.doi.org/10.1016/j.cej.2017.04.049>

This is a PDF file of an unedited manuscript that has been accepted for publication. As a service to our customers we are providing this early version of the manuscript. The manuscript will undergo copyediting, typesetting, and review of the resulting proof before it is published in its final form. Please note that during the production process errors may be discovered which could affect the content, and all legal disclaimers that apply to the journal pertain.



A facile strategy toward 3D hydrophobic composite resin network decorated with biological ellipsoidal structure rapeseed flower carbon for enhanced oils and organic solvents selective absorption

Jian Rong, Fengxian Qiu* , Tao Zhang*, Xiaoying Zhang, Yao Zhu, Jicheng Xu,

Dongya Yang and Yuting Dai

School of Chemistry and Chemical Engineering, Jiangsu University, Zhenjiang

212013, China.

Abstract

Fabrication of hydrophobic composite resin for enhancing oil-water or organic solvents-water separation applications has become increasingly attractive due to increasing industrial/domestic oily waste water and frequent oil accidents. In this work, firstly, carbonized pollen grain (PG) containing biological structure was prepared with rapeseed flower by the removing impurities, dehydration and calcinations. The morphologies of the synthesized PG show that they are ellipsoidal and hollow particles with length of *ca.* 30 μm , and pollen shell has a uniform network structure with an average pore size of 1.5 μm . Cross-sectional image of PG shows a palisade-like shell with the thickness of about 1 μm and vast pore canals. Outstanding BET surface area (379.98 $\text{m}^2 \text{g}^{-1}$) is achieved. Secondly, hydrophobic pollen grain

*Corresponding authors:

Tel./fax: +86 511 88791800.

E-mail: fxqiu@126.com (F. Qiu); zhangtaochem@163.com (T, Zhang)

(HPG) was prepared with PG by the surface activation and vinyltriethoxysilane (A151) modification under microwave-treated technique. The static contact angle for deionized water on HPG is 132° , indicating its excellent hydrophobic nature. Furthermore, a series of 3D hydrophobic composite resins (HCR) network decorated with different HPG content were prepared by the method of suspension polymerization under microwave conditions and benzoperoxide as initiator. Enhancing absorption capacities of 16.8 and 58.8 g g^{-1} to oils and organic solvents, respectively, are achieved. Pseudo-second-order and intra-particle diffusion kinetic models were employed for the corresponding organic solvents and oil absorption. This work represents a low cost, clean, and efficient route to prepare hydrophobic composite resin for absorption of oils and organic solvents with high performance, including absorption capacity, excellent selective separation performance on immiscible oil-water mixtures, good structural stability and reusability.

Keywords: Hydrophobic composite resins, 3D network polymer, Rapeseed flower, Biological structure, Absorption

1. Introduction

Frequent oil spill accidents and oil-contaminated industrial wastewater have caused severe environmental and ecological damage [1,2]. It also brings huge economic losses, including the loss of resource itself and the subsequent spending in dealing with the resource reclamation and environmental restoration [3,4]. Therefore, it is extremely urgent to design a low-cost, clean and effective oil-water separating materials for oil recovery and oily wastewater treatment.

Recently, various techniques have been employed to clean up or separate oils and organic pollutants from water. As traditional methods, oil booms, skimmers and barriers are frequently applied to treat oily wastewater. Nevertheless, low hydrophobic and oil-water selectivity of such materials severely limits the utilization efficiency and development [5]. Then, three-dimensional (3D) carbon-based aerogels, such as graphene sponge, carbon nanotube (CNT) sponge, carbon nanofiber (CNF) sponge and graphene/CNT hybrid foam [6-8], have attracted considerable interests due to its low cost, low apparent density, high porosity and specific surface area, and showed high absorption capacity for oil and organic solvent. However, the complicated preparation multi-steps, relatively high cost of starting materials (graphene or CNTs) and expensive equipment hindered the large-scale production of such aerogel materials for practical applications.

As an alternative, high oil-adsorbing resin has attracted much attention due to various outstanding performances. Oil-adsorbing acrylate resin is a polymer with low crosslinking degree and a three-dimensional (3D) network structure [9]. The polymer has a hydrophobic nature due to hydrophobic monomer [10]. Meanwhile, the oil-adsorbing acrylate resin also possess oil absorption variety, fast oil absorption rate, high oil retention capacity, recycling facilitate, and excellent reusability. What is more, the resin materials have a great advantage in dealing with the oil slick problem since it could float on the water surface for a long time. Here, the crosslinking density (swelling capability), porosity and storage space of acrylate resin play a pivotal role in oil absorption efficiency. Hence, many efforts have been taken to improve oil

absorption performance from above one or two aspects. Typically, Shan *et al.* [11] investigated the oil-absorption resins filled with polybutadiene with better swelling capability. Recently, Wang *et al.* [10] reported on improving oil absorption properties by the combination of biomorphic MgAl Layered Double Oxide and acrylic ester resin. Wang *et al.* [12] prepared the functionalized oil-absorption resins through polymerization from butyl methacrylate and kapok fiber. It can be drawn that the main purpose is to adjust binding force of covalent bond by altering single chemical cross-linking method, thereby possibly enhancing its oil absorption performance profile. Meanwhile, the incorporation of intact structure and firm fillers as frameworks could enhance mechanical strength in favor of reusability. In addition, appropriate biomass carbon materials were used instead of traditional synthetic materials with complicated preparation process, which has actually saved the production costs due to rich source, low-cost, easy preparation and renewable traits of natural products. However, despite the positive results achieved by many research groups, it was still not enough to ameliorate the absorption performance by unilateral improvement of acrylate resin.

In fact, lots of biological materials with excellent functional structure are inspired from nature, (such as butterfly wings [13], cotton fibers [14], pollen [15] and bamboo [16], *etc.*) which has caused great interest among researchers. Hereinto, pollen, with porous and hollow spherical structures, has been successfully replicated and has a wide range of applications due to its large pore volumes, high surface areas. These particular microstructures make them promising excellent absorption materials

with a larger storage space, which like a container for containing liquid. Compared with traditional introducing agent, pollen could not only make more developed porosity and adjust the degree of swelling, but also provide an extra oil storage space. In addition, a favorable macro 3D network structure could reduce the diffusion resistance of oil in resin thereby increasing the oil absorption rate. Moreover, pollen has a stable and uniform carbon skeleton make it have great advantage in controllable preparation process and environmental friendliness compared with the traditional chemical synthesis method. Then the introduction of chemical bonds between organic and inorganic phases could effectively enhance the interfacial interaction, which is a pivotal step to prepare the compatible composites leading the improvement of oil absorption performance and thermal stability [17].

With this in mind, herein, we report a new strategy for the synthesis of composite resin via the introduction of pollen grains into acrylate resin by the microwave-assisted suspension polymerization method. The simple pretreatment process of pollen grains and synthesis mechanism of composite resin was described in detail. In addition, the performances of the composite resin were studied in oils and organic solvents absorption. The resulting composite resin exhibited the characteristics of high absorption capacity, high selectivity and excellent reusability when it was employed as absorption material for various oils and organic solvents and collecting from the surface of water. Therefore, this study provides a new idea that a type of biomass material with a wide availability and oil storage space could be introduced into acrylate resin to improve the absorption performance by the combined

effect. To the best of our knowledge, no studies involving pollen grains and acrylate resin as oil absorption materials have been reported to date.

2. Experimental Section

2.1. Materials

All chemicals, including ethanol, nitric acid (HNO_3), sulfuric acid (H_2SO_4), formaldehyde, vinyltriethoxysilane (A151), butyl acrylate (BA), butyl methacrylate (BMA), polyvinyl alcohol (PVA), ethyl acetate and methylene-bis-acrylamide (MBA), were obtained from Sinopharm Chemical Reagent Co., Ltd (SCRC), which were all of analytical grade. Benzoperoxide (BPO) was purified by recrystallization from trichloromethane, dried at 60 °C and sealed preservation. Olive oil, soybean oil, sesame oil and golden arowana blend oil (cooking oil) were purchased from a supermarket in Jiangsu University. Diesel oil and pump oil were obtained from Sinopec. Rapeseed pollen purchased from Wang's Co., Ltd, Jiangsi Province, China. Deionized water was used for all experiments.

2.2. Preparation of carbonized pollen grains (PG) containing biological structure

Natural rapeseed flower pollen is composed of hard exine and tender core with complex biotic components, such as cellulose, hemicellulose, proteins, amino acids and nucleic acids. In order to obtain high surface area and perfect carbon skeleton, carbonized pollen grains (PG) was prepared as follows. The rapeseed flower pollen (5g) was immersed into ethanol solution (50 mL) for 4 h, followed by supersonic treatment for removing impurities. Then, the immersed pollen grains were filtered and washed with deionized water three times. In order to fix the morphology of carbon

skeleton, pollen grains were immersed in a mixed solution (60 mL) consisted of formaldehyde and ethanol (V/V, 1:1) for 10 min, followed by filtered and washed with deionized water three times. Then dehydration of the as-obtained pollen grains was carried out with sulfuric acid (50 mL, 12 mol L⁻¹) as a dehydrating agent under magnetic stirring at 80 °C for 4 h. The pollen grains were washed with deionized water and its pH value was adjusted to 7, dried in 80 °C for 20 h. Finally, the above resulting pollen grains were calcined at 600 °C for 2 h under the protection of nitrogen. The synthetic route of carbonized pollen grains (PG) containing biological structure is shown in Scheme 1.

2.3. Preparation of hydrophobic pollen grains (HPG)

PG (0.3 g) was loaded in a glass steamer to completely avoid contact with liquid. The glass steamer was then placed in a 100 mL Teflon-lined autoclave, at the bottom of which HNO₃ (0.3 mL, 65-68%) was loaded, sealed and heated at 120 °C for 5 h in an oven for steaming. In this elevated temperature process, the vaporized HNO₃ could react with the PG material quickly and the product was denoted as NPG. After steaming treatment, the NPG material was washed with deionized water and ethanol for three times and dried at 80 °C overnight. Then, NPG material (0.5g), ethanol (10 mL), water (10 mL), and A151 (coupling agent, 0.5 mL) were added into round bottom flask to react under microwave-treated at 80 °C (microwave power: 700 W) for 3 h. Finally, the pollen grains was washed with deionized water for three times and dried at 80 °C to obtain the hydrophobic pollen grains (expressed as HPG).

2.4. Preparation of 3D hydrophobic composite resin (HCR)

The 3D hydrophobic composite resin (HCR) was synthesized by the method of suspension polymerization under microwave conditions. Typically, a certain amount of polyvinyl alcohol (PVA, as dispersant) was dissolved with deionized water (20 mL) in a three-neck round bottom flask at 90 °C with a continuous magnetic stirring for 30 min. Then a mixture containing BA (6 g), BMA (4 g), MBA (as cross-link agent, 0.15 g), BPO (as initiator, 0.09 g), ethyl acetate (as porogen, 5 g), hydrophobic pollen grains (HPG) and deionized water (10 mL), was added drop and drop into above PVA aqueous solution in microwave reactor (Xianghu XH-100A, Beijing Xianghu Science and Technology Development Co., Ltd). Then the next four steps were implemented: 40 °C for 15 min (power = 600 W), 60 °C for 15 min (power = 600 W), 70 °C for 15 min (power = 600 W) and 80 °C for 2 h (power = 800 W), respectively. After cooling to room temperature naturally, the sample was washed with deionized water and ethanol three times and dried at 80 °C for 18 h to obtain composite resin. As a comparison, pure acrylate resin (PAR) also was prepared in the absence of HPG; and a series of 3D hydrophobic composite resin (HCR) network decorated with biological structure rapeseed flower carbon with different proportions ($m_{\text{HPG}} : m_{(\text{BA}+\text{BMA})} = 1\%$, 2%, 3%, 4%, 5% and 6%) were synthesized under the same conditions, denoted as HCR-1, HCR-2, HCR-3, HCR-4, HCR-5 and HCR-6, respectively.

2.5. Characterization

Surface morphology of the as-prepared samples were investigated by a scanning electron microscopy (SEM, S-4800, Hitachi, Tokyo, Japan) at accelerating voltage of 0.5-30 kV. X-ray diffraction (XRD) analysis was used to characterize the structure of

carbonized pollen grains. Radial scans were recorded in the reflection scanning mode from $2\theta = 5\text{--}80^\circ$ with a scanning rate of 7° min^{-1} . The surface area of as-prepared carbonized pollen grains was analyzed by nitrogen adsorption measurements, operated on a Micromeritics ASAP 2020 adsorption analyzer. The water contact angles (CA) were measured using $5 \mu\text{L}$ deionized water droplet at room temperature, which were conducted on a contact angle meter (Hitachi, CA-A), combined with a high speed camera. Water droplets were deposited directly at the top of the samples, and three measurements were performed per sample and averaged. Thermal stability of samples were characterized on a thermogravimetric analyzer (TG, STA 449 C, Netzsch, Germany) with a heating rate of $10^\circ \text{C min}^{-1}$ from 30 to 700°C under constant flow of nitrogen. Fourier transform infrared (FT-IR) spectra were performed on a FT-IR spectrometer (Nicolet, Nexus 670) in the range of $4000\text{--}400 \text{ cm}^{-1}$ via potassium bromide (KBr).

2.6. Absorption experiments

The composite resin was cut into 0.1 g and dipped into 11 kinds of oil or organic solvent (including trichloromethane, toluene, carbon tetrachloride, acetone and N,N-dimethylformamide (DMF), olive oil, soybean oil, sesame oil and golden arowana blend oil, diesel oil and pump oil) for 5 h. The absorption capacity, $q_e \text{ (g g}^{-1}\text{)}$, was calculated according to the following Equation (1):

$$q_e = \frac{m_e - m_0}{m_0} \quad (1)$$

where m_e and m_0 are the weight of the composite resin at absorption equilibrium and before absorption, respectively.

The absorption kinetic experiment was also carried out. The composite resin was immersed in carbon tetrachloride (CCl_4), trichloromethane (CHCl_3) and golden arowana blend oil for designated time intervals. The adsorbent was taken out and weighed. The absorption capacity, q_t (g g^{-1}), was calculated as following Equation (2):

$$q_t = \frac{m_t - m_0}{m_0} \quad (2)$$

where m_t (g) is the weight of the adsorbent after absorption at regular time t (min).

3. Results and discussion

3.1. Characterization of PG

Carbonized pollen grain (PG) containing biological structure was prepared with rapeseed flower by the removing impurities, dehydration and calcinations at $600\text{ }^\circ\text{C}$ for 2 h. Under low magnification (Figure 1A), it could be found clearly that all pollen grains have uniform particle size and homogeneous shape, indicating a successful retention of the pollen biological structure. This is mainly attributed to pretreatment process that it could clean impurities in pollen grains. Figure 1B presents the SEM image of PG under magnification. These pollen grains are ellipsoidal and hollow particles with length of *ca.* $30\text{ }\mu\text{m}$ [18], which could be as a storage space of adsorbate. Pollen shell shows a uniform network structure with an average pore size of $1.5\text{ }\mu\text{m}$, and this structure could be an excellent oily-liquid transmission channel [19]. Cross-sectional image of pollen grain shows a palisade-like shell with the thickness of about $1\text{ }\mu\text{m}$ and vast pore canals (Figure S1), which could provide a stable biological structure and high specific surface area. According to the XRD pattern given from Figure 1C, the prepared PG through the calcination process under the protection of

nitrogen only has a wide diffraction peak around $2\theta = 22^\circ$. The result is similar to previous results [7,20], indicating the formation of amorphous carbon.

It is well known that surface area is a significant factor for influencing the absorption capability of adsorbents [21]. Figure 1D exhibits a type IV isotherm with two hysteresis loops, indicating the presence of mesoporous and macroporous structure. The first hysteresis loop at a relatively low pressure (0.1-0.7) manifests the mesoporous structure existing in the prepared PG. Simultaneously; the other hysteresis loop at a high relative pressure (0.8-1.0) is mainly attributed to the macroporous structure corresponding to porous hollow pollen grains. The value of BET surface area is found to be $379.98 \text{ m}^2 \text{ g}^{-1}$. The pore size distribution is also investigated using BJH methods (as shown in inset Figure 1D). The PG has a narrow pore-size distribution with peak at *ca.* 4.56 nm, indicating the presence of mesoporous in the PG. Nitrogen adsorption-desorption isotherm does not show the information about macropores with sizes larger than 50 nm. Thus the macroporous structure was observed directly by SEM. High specific surface area and large pores could conducive to absorption process [22], which provides a larger contact surface and faster absorption rate.

3.2. Hydrophobic property of NPG and HPG

HPG was prepared with PG by the surface activation and vinyltriethoxysilane (A151) modification under microwave-treated technique. For comparison, NPG was also fabricated without modification. Contact angle measurements were conducted in NPG and HPG with deionized water using sessile drop method (Figure 2). Thin layers

of the modified carbonized pollen grains were prepared by fixing the power on a glass slide with the help of a double adhesive tape. From the Figure 2A, it can be seen that water drop was rapidly sucked down into NPG once the droplets had contact with the surface, and the static contact angle for water drop could not be measured immediately due to the rapid penetration. On the contrary, the static contact angle for deionized water on HPG was measured to be 132° , indicating its excellent hydrophobic property (Figure 2B). Figure 2C presents interactive impact that the droplet could remain in the surface of HPG within 20 seconds. It is interesting that water droplet stays in the surface of sample without significant change, suggesting excellent stability of hydrophobicity. Compared with NPG, this is mainly because the surface of HPG formed a compact Si-O-Si hydrophobic layer after the modification with coupling agent vinyltriethoxysilane (A151) [23]. Figure S2 depicts the FT-IR spectra of PG, NPG and HPG, which indicating that the hydroxyl groups on the pollen grain play a key role in the preparation of hydrophobic pollen grain surface [24]. Compared with PG and NPG, the HPG shows three new adsorption peaks at 1133.27, 792.49 and 467.82 cm^{-1} , which could be ascribed to the Si-O-Si antisymmetric stretching vibration, symmetric stretching vibration and bending vibration, respectively [25].

3.3. Morphology and thermal stability of composite resin

A series of 3D hydrophobic composite resin (HCR) were synthesized with different proportions ($m_{\text{HPG}} : m_{(\text{BA}+\text{BMA})} = 1\%, 2\%, 3\%, 4\%, 5\%$ and 6%) by the method of suspension polymerization, denoted as HCR-1, HCR-2, HCR-3, HCR-4,

HCR-5 and HCR-6, respectively. For comparison, pure acrylate resin (PAR) was prepared in the absence of HPG. From Figure 3A, it was found that the surface of the PAR is smooth. Compared with the pure acrylate resin (PAR), it could be clearly seen that the surface of composite resin HCR-4 becomes rough (Figure 3B). This result also shows that the introduction of pollen grains has a direct impact on internal structure of pure acrylate resin PAR. The unique 3D network and porous structure are favorable to efficient improving the oil-adsorbing properties of composite resin.

TGA and DSC curves PAR and HCR-4 are shown in Figure 3(C and D). From Figure 3C, the apparent weight loss of PAR is observed in the temperature range of 320 °C to 420 °C (a penetrating endothermic peak at 386.7 °C), while the 345 to 430 °C (a penetrating endothermic peak at 391.4 °C) in Figure 3D. The result shows that the thermal stability of composite resin HCR-4 is improved after the introduction of rapeseed flower carbon.

3.4. Synthesis of composite resin and absorption mechanism

A simple synthesis mechanism of composite resin is shown in Figure 4. The HNO₃ steam treatment was meaningful to make hydroxyl and carbonyl (or carboxyl) groups (Figure S2) expose on the surface of pollen grains for the subsequent graft polymerization reaction. Afterwards, with the help of initiator BPO, the H⁺ of hydroxyl or carboxyl groups on the surface of pollen grains containing biological structure could be taken away and consequently generate radicals (Step 1). Meanwhile, the co-monomer molecules (BA and BMA) were transformed into a chain with the fracture of carbon-carbon double bonds and subsequently formed polymerized

acrylate resin due to the presence of BPO and ethyl acetate (Step 2). Furthermore, the radicals of resin chain end also have a trend to accept the radicals on the pollen grain surface, which will make the as-obtained sample structure more stable since it was linked by extra chemical bond rather than a simple physical mixing. Finally, an interpenetrating polymer with 3D network structure was obtained due to the effect of cross-link agent (MBA) (Step 3). Interestingly, there is hardly any impact on the biological and porous structures of pollen grains throughout the synthetic process. After polymerization, the composite resin with biological structure, 3D network and interconnected pore structure could provide smooth channels for organic solvent or oil rapid diffusion and storage. The driving force of absorption is attributed to Van der Waals and capillary force interactions between the composite resin and the oil molecules [10]. Then composite resin will achieve a high absorption capacity via a limited swelling process (Step 4) without destroying the overall biological structure, 3D network and properties.

3.5. Oils and organic solvents absorption

A comparative study for carbon tetrachloride absorption was carried out over the prepared composite resin and the results are shown in Figure 5. As can be seen from Figure 5, the carbon tetrachloride absorption of HCR material is significantly improved as compared with PAR. It could be noted that absorption capacity of HCR material increases firstly and then decreases with the increasing of the pollen grains proportion. Among the prepared resins, HCR-4 has the highest absorption capacity, *i.e.* 58 g g^{-1} , which is about 2 times larger than the counterpart pure acrylate resin

(PAR). Judging from the structure of the composite resins, it is thought that the 3D network structure and porous pollen grains are accountable for the oil absorption capacity variation since the absorption mechanism is dominated by physical storage of oil in the pollen grains and capillary force. Then high BET specific surface area of pollen grains could provide more absorption space. Nevertheless, excess pollen grains made oil absorption capacity of composite resin decreases, which may be caused by the reduction of oil retention capacity on account of excessive proportion of pollen grains [26]. Based on above results, HCR-4 was fixed as optimum oil absorbent for the rest absorption experiments.

For a detailed study of the oil-absorbing properties of composite resin, several absorption experiments using carbon tetrachloride as the target absorbate were performed, as shown in Figure 6. From the Figure 6(A and B), it is found that HCR exhibits excellent swelling properties during absorption process [27]. Absorption performance of composite resin is a swelling process, in which oil molecules permeate into 3D channel continually to give it rise to swelling [11]. From this view to speculate, chemical crosslinking intensity could play an important role in oil absorption. The undue tightness could inhibit the expansion of the resin, and excessive low crosslinking intensity could reduce the network structure stability and oil retention capacity. Hence, with an appropriate addition of pollen grains, an improvement of oil absorption capacity could be achieved due to advisable crosslinking intensity. This speculation is in accordance with the variation trend of absorption capacity (as shown in Figure 5) owing to adding different amount of pollen

grains. More serious, the synthesized pure acrylate resin (PAR) from co-monomers is likely to collapse after swelling [28]. Therefore, the introduction of pollen grains with extra skeleton can strengthen the mechanical stability. From the Figure 6C, it is found that the volume of composite resin after absorption is close to 20 times compared with before oil absorption, and 3D network structure of composite still kept intact.

Figure 6(D and E) show a rapid oil absorption process of the composite resin. It was clearly seen that the composite resin was simply immersed in a carbon tetrachloride solution dyed red combined with gently wipe (Figure 6D). The whole absorption process took approximately 5 seconds. Then it was noteworthy that carbon tetrachloride was quickly and completely absorbed from the glass culture dish. Therefore, the composite resin could have great potential to remove toxic oily liquid in emergency.

A further investigation was used to test the performance of the oil-water selective separation for composite resin, as shown in Figure 6(F-I). When the water droplet was dropped on the composite resin, it still stood on the surface with the sphere shape during 30 seconds. Nevertheless, it was observed that carbon tetrachloride was immediately absorbed (Figure 6F). Considering its hydrophobicity, the above experiment powerfully demonstrated that the composite resin could be an excellent oil-water separating agent. Afterwards, about 5 mL of carbon tetrachloride was added in 25 mL deionized water in a culture dish under quiescent conditions (Figure 6G). As shown in Figure 6H, when the composite resin was dipped into oil/water system, it immediately absorbed the oil phase and started to swell under the action of

hydrophobicity, Van der Waals and capillary force. After about 15 seconds, a result showed that no obvious oil phase floated on the surface of water, indicating the high separation efficiency (Figure 6I). A complete selective oil-water separation process was provided in Figure S3. Then Figure S4(A-E) showed the images of the removal process of carbon tetrachloride (labeled by Sudan III) under water. When the bulk HCR-4 was inserted into water by an external force approach carbon tetrachloride, the carbon tetrachloride droplet could be immediately sucked up and removed. For organic solvents such as acetone and DMF, they are miscible with water. As shown in Figure S4F, when the HCR-4 was immersed in mixture of acetone and water, it was reflective because of the existence of air cushion between water and the HCR-4 surface, which means that the interaction between water and the hydrophobic composite resin is very weak [7]. Unfortunately, the air cushion acts as a repulsive layer for acetone organic molecules, thus forming a HCR-4/air cushion/acetone interface [19]. The air cushion reduces the contact area between the HCR-4 and the acetone organic molecules, thereby further the absorption of HCR-4 on acetone will be hindered, which is similar to the self-cleaning function of lotus leaf [29]. Hence, the oil-water separation experiments demonstrated that the as-prepared HCR-4 can be applied to separate immiscible oil-water mixtures effectively.

In order to study the absorption capacity of as-prepared composite resin on different oily liquid, a series of oil absorption experiment were carried out under the same conditions. Figure 7 shows the maximum oil absorption capacity of HCR-4 for common organic solvents (Figure 7A) and oils (Figure 7B), respectively. It is found

that the absorption capacities of organic solvents are much bigger than those of the selected oils. The absorption capacity of the composite resin on organic solvents and oils are ranged from 25.1 to 58.8 g g⁻¹ and 7.8 to 16.8 g g⁻¹, respectively. 3D porous network structure of composite resin could provide large accessible surface area and high porosity. It is expected that 3D network structure, strong hydrophobicity and extra storage space of hollow pollen grains could have a combined or synergistic effect on absorbing organic solvents and oils. In addition, it is worth noting that the absorption capacity of HCR-4 is much higher to that of many other reported oil absorption materials (Table S1), and it exhibits different degrees of swelling to various absorbates (Figure S5). The absorption capacities of as-prepared HCR-4 for these selected organic solvents are mainly affected by the density of the organic solvent [6,7]. For example, the absorption capacity of the HCR-4 for carbon tetrachloride (density = 1.60 g cm⁻³) is 58.8 g g⁻¹ and for acetone (density = 0.785 g cm⁻³) is 32.7 g g⁻¹. In addition, hydrophobic composite resin also has the selectivity of organic solvents to some extent. For example, the absorption capacity of the HCR-4 for DMF (density = 0.948 g cm⁻³, which is higher than the density of acetone) is 25.1 g g⁻¹. Hence, it could be interpreted that the polarities (DMF > acetone) of organic solvents were different, thereby further affecting the swelling degree of the composite resin [30]. It is not difficult to find that the degree of swelling and absorption capacity exhibited positive correlation. From the above absorption performances on organic solvents and various oils, composite resin has great potential to be a good absorbent and can be applied for the treatment of oily wastewater, the removal of mechanical

resid, the cleaning of kitchen grease and so on.

3.6. Kinetic study

The absorption kinetics experiments were employed to explore the absorption mechanism on the selected samples. The relationship of the absorption capacity of carbon tetrachloride, trichloromethane and golden arowana blend oil on HCR-4 versus absorption time is shown in Figure 8. It is found that the trends of carbon tetrachloride and trichloromethane show a relatively rapid absorption process in previous period, followed a gradually slow absorption process until reached saturation. The trend of golden arowana blend oil, by contrast, exhibits a relatively stable growth until a saturation concentration in composite resin. The absorption equilibrium was reached at about 240 min. The absorption kinetic of absorbent is most frequently modeled by using the pseudo-first-order, pseudo-second-order, and intraparticle diffusion kinetic model.

A linear form of pseudo-first-order model was described by the following Equation (3) [31,32]:

$$\ln(q_e - q_t) = \ln q_e - k_1 t \quad (3)$$

where q_e and q_t are the absorption capacity (g g^{-1}) at equilibrium and at any instant of time (min), respectively, and k_1 is the rate constant of pseudo-first-order absorption (min^{-1}).

The pseudo-second-order kinetics may be expressed as the following Equation (4) [33,34]:

$$\frac{t}{q_t} = \frac{1}{k_2 q_e^2} + \frac{1}{q_e} t \quad (4)$$

where k_2 is the equilibrium rate constant of pseudo-second-order absorption ($\text{g} \cdot (\text{g} \cdot \text{min})^{-1}$).

The intra-particle diffusion kinetic model was borrowed, which model is expressed as the following Equation (5) [35]:

$$q_t = k_p t^{1/2} + C \quad (5)$$

where C is the intercept and k_p is the intraparticle diffusion rate constant ($\text{g} \cdot \text{min}^{-1}$).

The intra-particle diffusion kinetic model based on the theory or equation proposed by Weber and Morris was tested [36], which is an empirically functional relationship.

The computed values for C , q_e , the calculated value of absorption capacity (q_{cal}) and the correlation coefficient (R^2) are summarized in Table 1. Based on correlation coefficients, the experiment data kinetic model of carbon tetrachloride (0.992) and trichloromethane (0.993) fit well with the pseudo-second-order while golden arowana blend oil (0.930) is more in line with the intra-particle diffusion kinetic model. Besides, the q_{cal} of carbon tetrachloride, trichloromethane and golden arowana blend oil according to corresponding kinetic model (60.4, 43.3 and 7.53 $\text{g} \cdot \text{g}^{-1}$) are quite close to the experiment values ($q_e = 58.8, 42.3$ and $7.80 \text{ g} \cdot \text{g}^{-1}$). In terms of above result, a tentative mechanism of oils and organic solvents absorption for composite resin is put forward as follows. Organic solvents absorption could be dominated by chemical absorption that organic solvents molecules could have a strong binding force with lipophilic group existing in composite resin. Therefore, a relatively rapid oil absorption rate and swelling rate are exhibited in previous period since abundant lipophilic groups could be contested. Nevertheless, oils absorption could be controlled

by various factors, which could contain the density, polar, viscosity of oil and so forth [37,38]. Compared with organic solvent, it is well known that oil macromolecules have a relatively weak force with the polymers.

3.7. Reusability of the composite resin

Furthermore, oil absorption capacities of the composite resin (HCR-4) after five cycles of the absorption process for carbon tetrachloride, trichloromethane and golden arowana blend oil are shown in Figure 9. It is worth noting that the absorbed oil and organic solvents could be easily removed from composite resin by washed with ethanol combining subsequent vacuum drying (Figure S6), and the resultant samples could be reused in the next absorption-regeneration cycle. Interestingly, the increase in the cycles almost has no significant influence on the absorption capacity in the first five cycles, which implies excellent stability and relatively long service life of composite resin. Compared with the PAR (Figure 5), the absorption capacity of the HCR is improved obviously. The absorption capacity changes little after 5 absorption cycles, which mainly attribute to the excellent structure stability due to the introduction of appropriate pollen particles. The high absorption capacity and excellent structural stability endow the material to be an ideal candidate to remove a variety of oils and organic solvents in practical applications.

4. Conclusions

In summary, 3D hydrophobic composite resin (HCR) network containing ellipsoidal-like rapeseed flower carbon has been successfully synthesized by the method of suspension polymerization under microwave conditions for the first time.

The HCR demonstrates excellent oils/organic solvents absorption performance, selective separation performance on immiscible oil-water mixtures as well as a high absorption capacity of 58.8 g g⁻¹. Besides, organic solvents and oils absorption processes followed pseudo-second-order and intra-particle diffusion kinetic models, respectively, and the absorption mechanism was discussed in detail, as well as absorption capacity changes little after 5 absorption cycles. Given its excellent reusability and durability, the concept presented herein can be further expanded to facile preparation of 3D hydrophobic composite resin by the introduction of functional biomass materials for high-performance application in absorptions, oils-water separation, organic solvents-water, and waste water treatment containing dyes and heavy metal ion.

Acknowledgements

This work was financially supported by National Nature Science Foundation of China (U1507115), Natural Science Foundation of Jiangsu Province (BK20160500 and BK20161362), Jiangsu Planned Projects for Postdoctoral Research Funds (1601016A) and Scientific Research Foundation for Advanced Talents of Jiangsu University (15JDG142).

References

- [1] W. Wan, R. Zhang, W. Li, H. Liu, Y. Lin, L. Li, Y. Zhou, Graphene-carbon nanotube aerogel as an ultra-light, compressible and recyclable highly efficient absorbent for oil and dyes, *Environ. Sci.: Nano* 3 (2016) 107-113.
- [2] C.-H. Xue, Y.-R. Li, J.-L. Hou, L. Zhang, J.-Z. Ma, S.-T. Jia, Self-roughened

- superhydrophobic coatings for continuous oil-water separation, *J. Mater. Chem.A* 3 (2015) 10248-10253.
- [3] J. Wu, N. Wang, Y. Zhao, L. Jiang, Simple synthesis of smart magnetically driven fibrous films for remote controllable oil removal, *Nanoscale* 7 (2015) 2625-2632.
- [4] G. Wang, Y. He, H. Wang, L. Zhang, Q. Yu, S. Peng, X. Wu, T. Ren, Z. Zeng, Q. Xue, A cellulose sponge with robust superhydrophilicity and under-water superoleophobicity for highly effective oil/water separation, *Green Chem.* 17 (2015) 3093-3099.
- [5] S. Yu, Z. Guo, Superhydrophobic surfaces based on polypyrrole with corrosion resistance and the separation of oil/water mixture properties, *RSC Adv.* 5 (2015) 107880-107888.
- [6] S. Yang, L. Chen, L. Mu, B. Hao, P.-C. Ma, Low cost carbon fiber aerogel derived from bamboo for the adsorption of oils and organic solvents with excellent performances, *RSC Adv.* 5 (2015) 38470-38478.
- [7] J. Zhang, B. Li, L. Li, A. Wang, Ultralight, compressible and multifunctional carbon aerogels based on natural tubular cellulose, *J. Mater. Chem.A* 4 (2016) 2069-2074.
- [8] R. Du, Q. Feng, H. Ren, Q. Zhao, X. Gao, J. Zhang, Hybrid-dimensional magnetic microstructure based 3D substrates for remote controllable and ultrafast water remediation, *J. Mater. Chem.A* 4 (2016) 938-943.
- [9] G.R. Shan, P.Y. Xu, Z.X. Weng, Z.M. Huang, Oil - absorption function of physical crosslinking in the high - oil - absorption resins, *J. Appl. Polym. Sci.* 90 (2003)

3945-3950.

- [10] Y. Wang, Q. Li, L. Bo, X. Wang, T. Zhang, S. Li, P. Ren, G. Wei, Synthesis and oil absorption of biomorphic MgAl Layered Double Oxide/acrylic ester resin by suspension polymerization, *Chem. Eng. J.* 284 (2016) 989-994.
- [11] G.R. Shan, P.Y. Xu, Z.X. Weng, Z.M. Huang, Synthesis and properties of oil absorption resins filled with polybutadiene, *J. Appl. Polym. Sci.* 89 (2003) 3309-3314.
- [12] J. Wang, Y. Zheng, A. Wang, Preparation and properties of kapok fiber enhanced oil sorption resins by suspended emulsion polymerization, *J. Appl. Polym. Sci.* 127 (2013) 2184-2191.
- [13] Z. Mu, X. Zhao, Z. Xie, Y. Zhao, Q. Zhong, L. Bo, Z. Gu, In situ synthesis of gold nanoparticles (AuNPs) in butterfly wings for surface enhanced Raman spectroscopy (SERS), *J. Mater. Chem.B* 1 (2013) 1607-1613.
- [14] X. Tao, L. Dong, X. Wang, W. Zhang, B.J. Nelson, X. Li, B₄C-nanowires/carbon-microfiber hybrid structures and composites from cotton T-shirts, *Adv. Mater.* 22 (2010) 2055-2059.
- [15] Y. Xia, W. Zhang, Z. Xiao, H. Huang, H. Zeng, X. Chen, F. Chen, Y. Gan, X. Tao, Biotemplated fabrication of hierarchically porous NiO/C composite from lotus pollen grains for lithium-ion batteries, *J. Mater. Chem.* 22 (2012) 9209-9215.
- [16] X. Tao, J. Du, Y. Li, Y. Yang, Z. Fan, Y. Gan, H. Huang, W. Zhang, L. Dong, X. Li, TaC nanowire/activated carbon microfiber hybrid structures from bamboo fibers, *Adv Energy Mater.* 1 (2011) 534-539.

- [17] C.-H. Tseng, H.-B. Hsueh, C.-Y. Chen, Effect of reactive layered double hydroxides on the thermal and mechanical properties of LDHs/epoxy nanocomposites, *Compos. Sci. Technol.* 67 (2007) 2350-2362.
- [18] K. Tian, X.-X. Wang, H.-Y. Li, R. Nadimicherla, X. Guo, Lotus pollen derived 3-dimensional hierarchically porous NiO microspheres for NO₂ gas sensing, *Actuat. B-Chem.* 227 (2016) 554-560.
- [19] F. Liu, R. Lu, Q. Pan, Juncus Pith: a versatile material for automatic and continuous separation of various oil–water mixtures, *ACS Sustainable Chem. Eng.* 5 (2017) 922-928.
- [20] Y.-Q. Li, Y.A. Samad, K. Polychronopoulou, S.M. Alhassan, K. Liao, Carbon aerogel from winter melon for highly efficient and recyclable oils and organic solvents absorption, *ACS Sustainable Chem. Eng.* 2 (2014) 1492-1497.
- [21] X. Zhang, J. Liu, S.J. Kelly, X. Huang, J. Liu, Biomimetic snowflake-shaped magnetic micro-/nanostructures for highly efficient adsorption of heavy metal ions and organic pollutants from aqueous solution, *J. Mater. Chem.A* 2 (2014) 11759-11767.
- [22] J. Deng, B. Yang, C. Chen, J. Liang, Renewable eugenol-based polymeric oil-absorbent microspheres: preparation and oil absorption ability, *ACS Sustainable Chem. Eng.* 3 (2015) 599-605.
- [23] A. Kumar, M. Petrič, B. Kričej, J. Žigon, J. Tywoniak, P. Hajek, A.S. Škapin, M. Pavlič, Liquefied-wood-based polyurethane–nanosilica hybrid coatings and hydrophobization by self-assembled monolayers of orthotrichlorosilane (OTS),

ACS Sustainable Chem. Eng. 3 (2015) 2533-2541.

- [24] J. Li, L. Yan, Y. Zhao, F. Zha, Q. Wang, Z. Lei, One-step fabrication of robust fabrics with both-faced superhydrophobicity for the separation and capture of oil from water, *Phys. Chem. Chem. Phys.* 17 (2015) 6451-6457.
- [25] C. Feng, D. Li, Morphology-controlled synthesis of SiO₂ hollow microspheres using pollen grain as a biotemplate. *Biomed. Mater.* 4 (2009) 025009.
- [26] W. Zhang, M. Liu, Y. Liu, R. Liu, F. Wei, R. Xiao, H. Liu, 3D porous poly(l-lactic acid) foams composed of nanofibers, nanofibrous microspheres and microspheres and their application in oil-water separation, *J. Mater. Chem. A* 3 (2015) 14054-14062.
- [27] S. Hu, J. Gu, F. Jiang, Y.-L. Hsieh, Holistic rice straw nanocellulose and hemicelluloses/lignin composite films, *ACS Sustainable Chem. Eng.* 4 (2016) 728-737.
- [28] L. Yang, B. Bai, C. Ding, H. Wang, Y. Suo, Synthesis and properties of the rapeseed meal-grafted-poly(methyl methacrylate-co-butyl acrylate) oil-absorbents, *RSC Adv.* 6 (2016) 9507-9517.
- [29] S. Wang, K. Liu, X. Yao, L. Jiang, Bioinspired surfaces with superwettability: new insight on theory, design, and applications, *Chem. Rev.* 115 (2015) 8230-8293.
- [30] Y. Du, P. Fang, J. Chen, X. Hou, Synthesis of reusable macroporous St/BMA copolymer resin and its absorbency to organic solvent and oil, *Polym. Adv. Technol.* 27 (2016) 393-403.

- [31] R. Leyva-Ramos, J. Rivera-Utrilla, N. Medellin-Castillo, M. Sanchez-Polo, Kinetic modeling of fluoride adsorption from aqueous solution onto bone char, *Chem. Eng. J.* 158 (2010) 458-467.
- [32] T. Zhang, Q. Li, Y. Liu, Y. Duan, W. Zhang, Equilibrium and kinetics studies of fluoride ions adsorption on $\text{CeO}_2/\text{Al}_2\text{O}_3$ composites pretreated with non-thermal plasma, *Chem. Eng. J.* 168 (2011) 665-671.
- [33] Y.-S. Ho, Second-order kinetic model for the sorption of cadmium onto tree fern: a comparison of linear and non-linear methods, *Water Res.* 40 (2006) 119-125.
- [34] Y.-S. Ho, G. McKay, The kinetics of sorption of divalent metal ions onto sphagnum moss peat, *Water Res.* 34 (2000) 735-742.
- [35] H. Zaghouane-Boudiaf, M. Boutahala, Kinetic analysis of 2, 4, 5-trichlorophenol adsorption onto acid-activated montmorillonite from aqueous solution, *Int. J. Miner. Process.* 100 (2011) 72-78.
- [36] A.L. Ahmad, C.Y. Chan, S.R. Abd Shukor, M.D. Mashitah, Adsorption kinetics and thermodynamics of β -carotene on silica-based adsorbent, *Chem. Eng. J.* 148 (2009) 378-384.
- [37] Y. Jin, P. Jiang, Q. Ke, F. Cheng, Y. Zhu, Y. Zhang, Superhydrophobic and superoleophilic polydimethylsiloxane-coated cotton for oil-water separation process: An evidence of the relationship between its loading capacity and oil absorption ability, *J. Hazard. Mater.* 300 (2016) 175-181.
- [38] J. Chen, P. Fang, Y. Du, X. Hou, Synthesis and properties of lipophilic polyelectrolyte styrene/butyl methacrylate/stearyl methacrylate resin as

absorbent materials for organic solvents and oils, *Colloid. Polym. Sci.* 294 (2016)

119-125.

ACCEPTED MANUSCRIPT

Scheme 1 Schematic illustration on the synthetic route of carbonized pollen grains (PG) containing biological structure.

Figure 1. SEM images of at different magnifications (A and B), XRD pattern (C) and nitrogen adsorption-desorption isotherm and inset pore size distributions (D) of PG.

Figure 2. Hydrophobicity characterization: water contact angle image of the NPG (A) and HPG (B); photographs showing the interaction of a water droplet with the HPG in 20 s (C).

Figure 3. SEM images of (A) PAR and (B) HCR-4; TGA and DSC curves of (C) PAR and (D) HCR-4 obtained in an N₂ atmosphere.

Figure 4. Schematic illustration of the synthesis and absorption mechanism of composite resin network decorated with biological structure rapeseed flower carbon.

Figure 5. Carbon tetrachloride absorption of PAR and HCR materials.

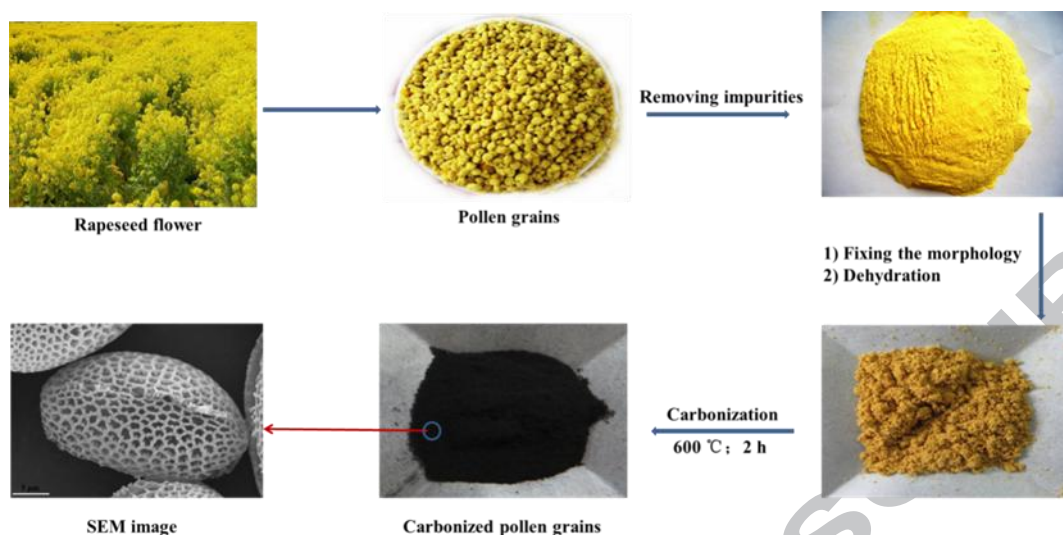
Figure 6. Images of the experiment process: (A, B and C) the absorption of carbon tetrachloride and swelling of composite resin; (D and E) the rapid absorption process of composite resin on carbon tetrachloride; (F-I) selective absorption for

oil-water and removal of carbon tetrachloride from water surface by the HCR-4, carbon tetrachloride was labeled by Sudan III for clarity.

Figure 7. Absorption capacities of HCR-4 for selected (A) organic solvents and (B) oils.

Figure 8. The time-dependent absorption capacity of carbon tetrachloride, trichloromethane and golden arowana blend oil on HCR-4; Black and red solid line were fitted from pseudo-second-order kinetic model, and blue solid line was fitted from intraparticle diffusion kinetic model.

Figure 9. Recyclability and regeneration of HCR-4 for the absorption of Carbon tetrachloride, trichloromethane and golden arowana blend oil.



Scheme 1 Schematic illustration on the synthetic route of carbonized pollen grains

(PG) containing biological structure.

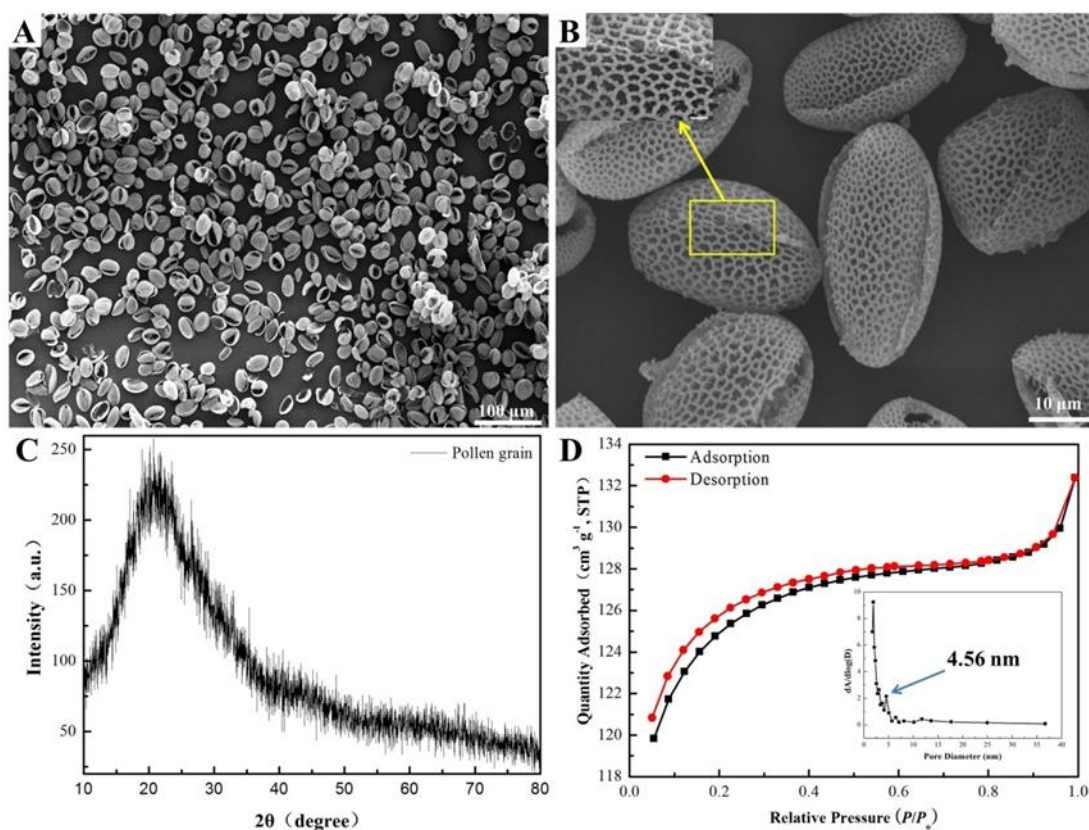


Figure 1. SEM images of at different magnifications (A and B), XRD pattern (C) and nitrogen adsorption-desorption isotherm and inset pore size distributions (D) of PG.

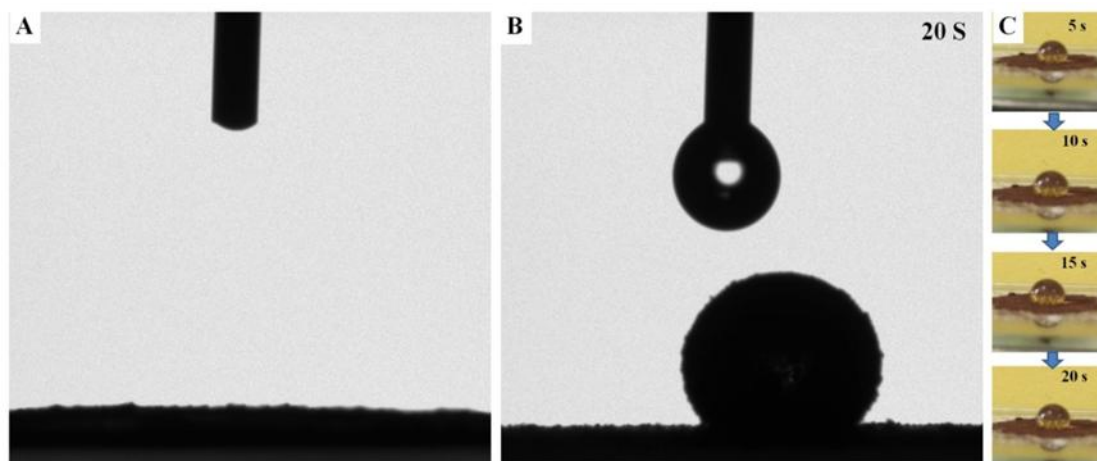


Figure 2. Hydrophobicity characterization: water contact angle image of the NPG (A) and HPG (B); photographs showing the interaction of a water droplet with the HPG in 20 s (C).

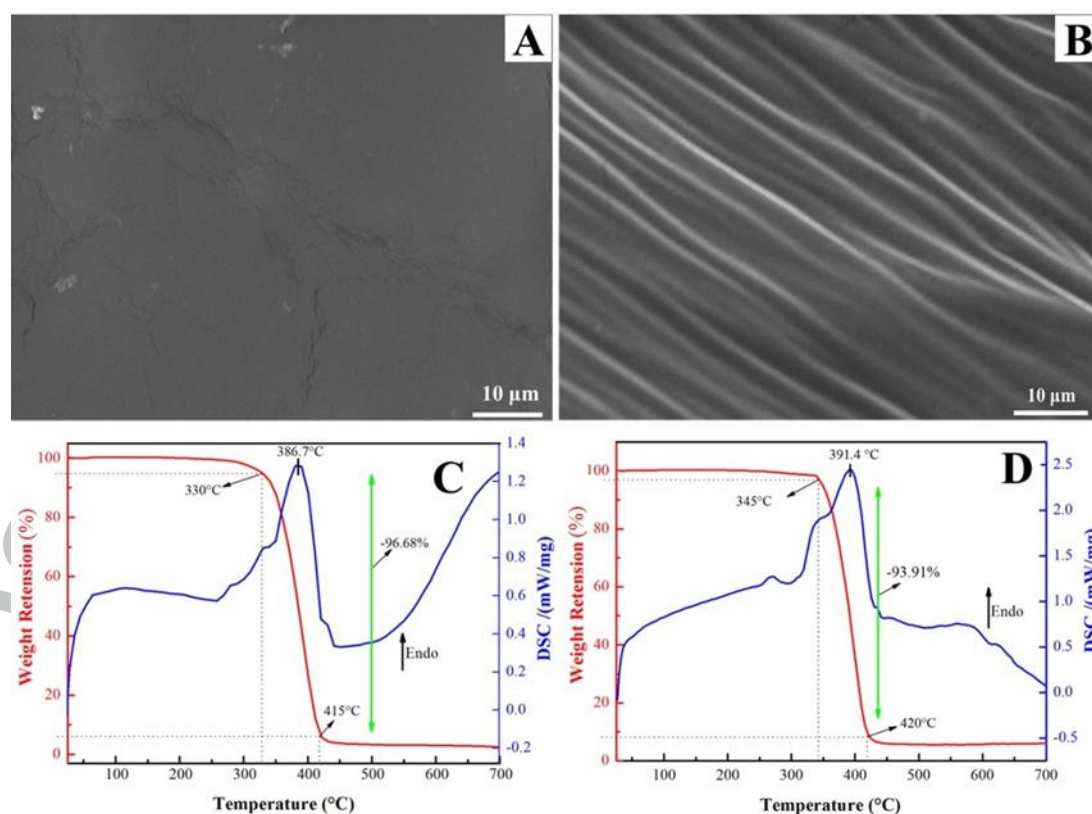


Figure 3. SEM images of (A) PAR and (B) HCR-4; TGA and DSC curves of (C) PAR and (D) HCR-4 obtained in an N_2 atmosphere.

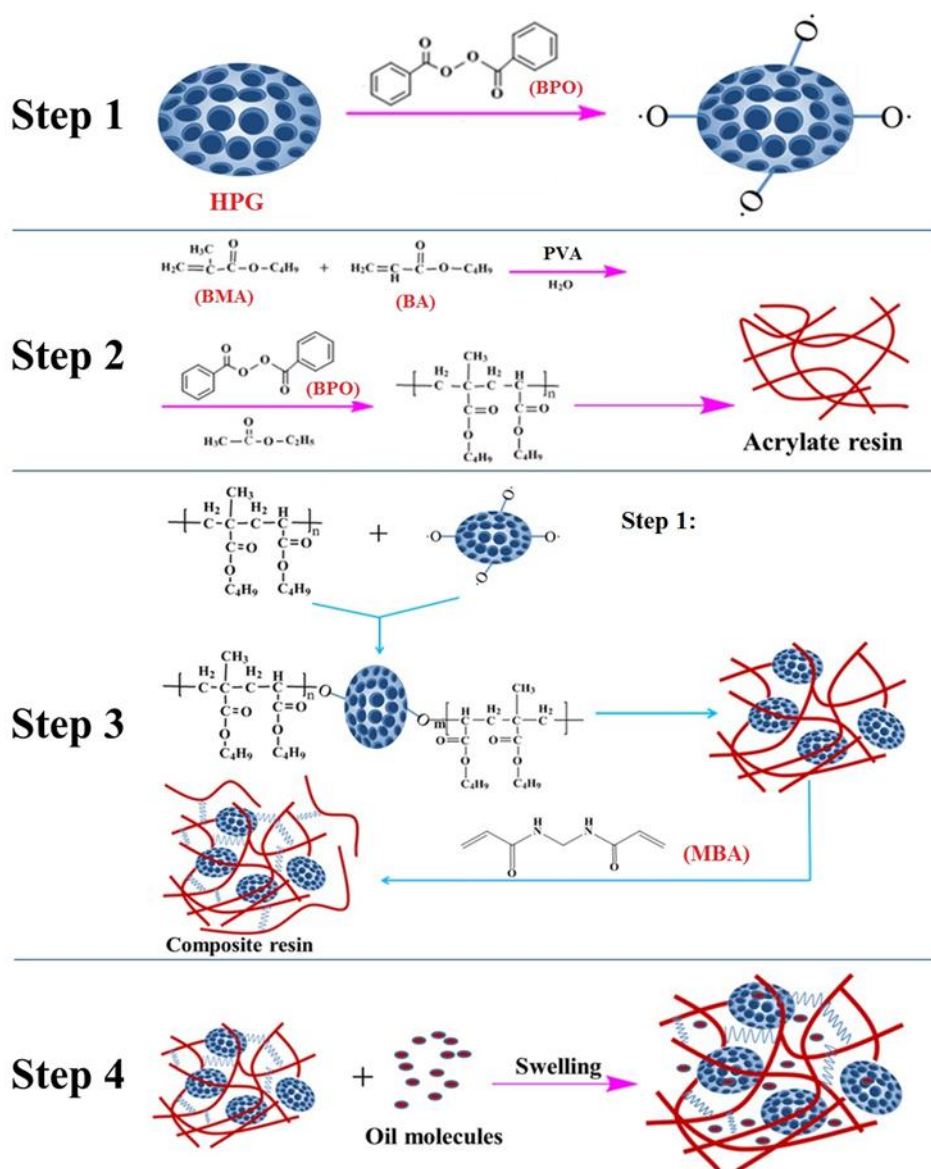


Figure 4. Schematic illustration of the synthesis and absorption mechanism of composite resin network decorated with biological structure rapeseed flower carbon.

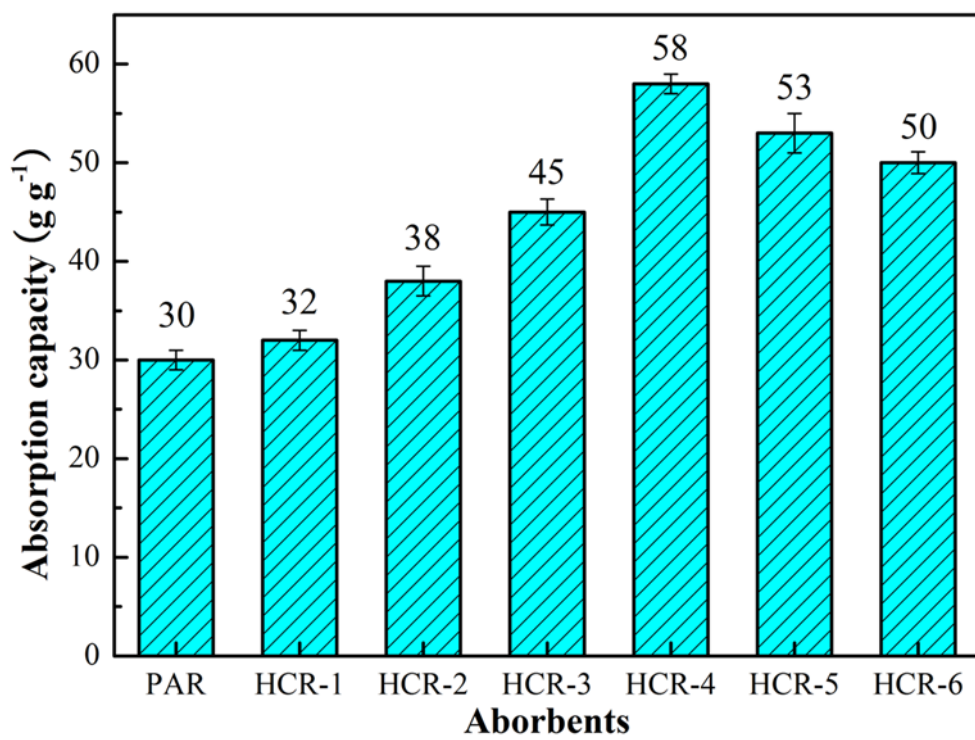


Figure 5. Carbon tetrachloride absorption of PAR and HCR materials.

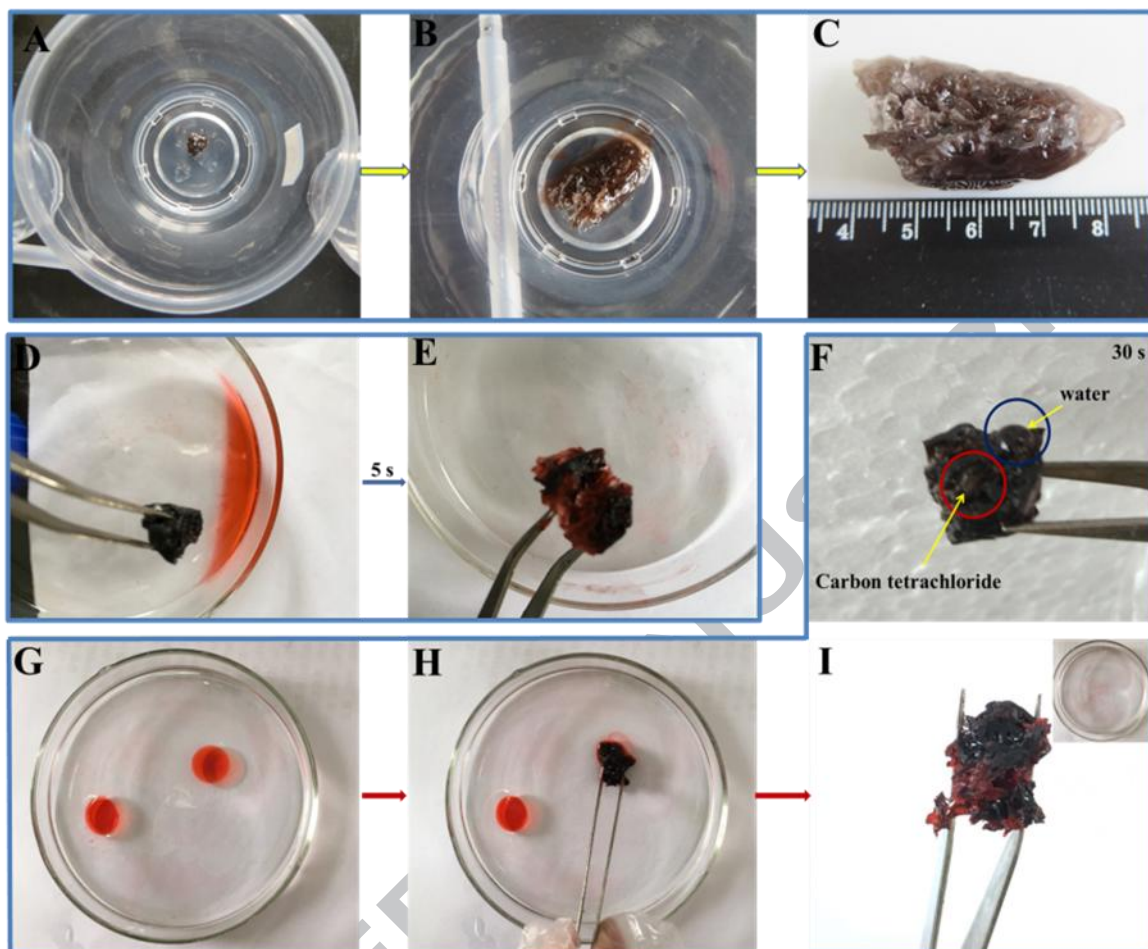


Figure 6. Images of the experiment process: (A, B and C) the absorption of carbon tetrachloride and swelling of composite resin; (D and E) the rapid absorption process of composite resin on carbon tetrachloride; (F-I) selective absorption for oil-water and removal of carbon tetrachloride from water surface by the HCR-4, carbon tetrachloride was labeled by Sudan III for clarity.

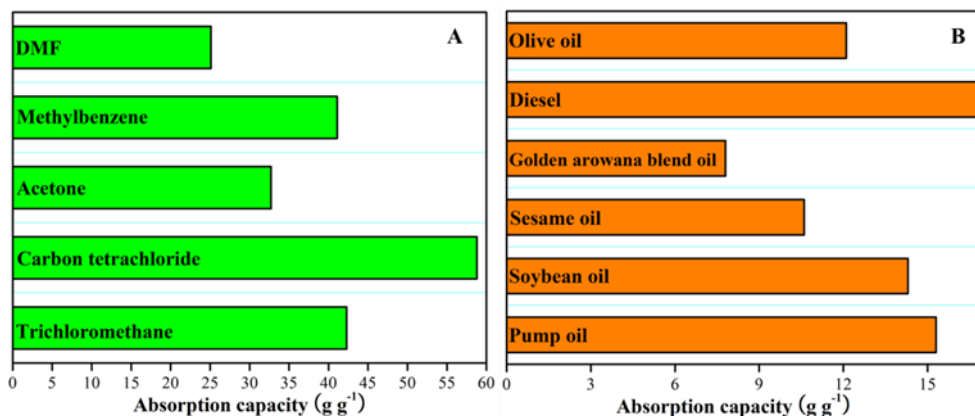


Figure 7. Absorption capacities of HCR-4 for selected (A) organic solvents and (B) oils.

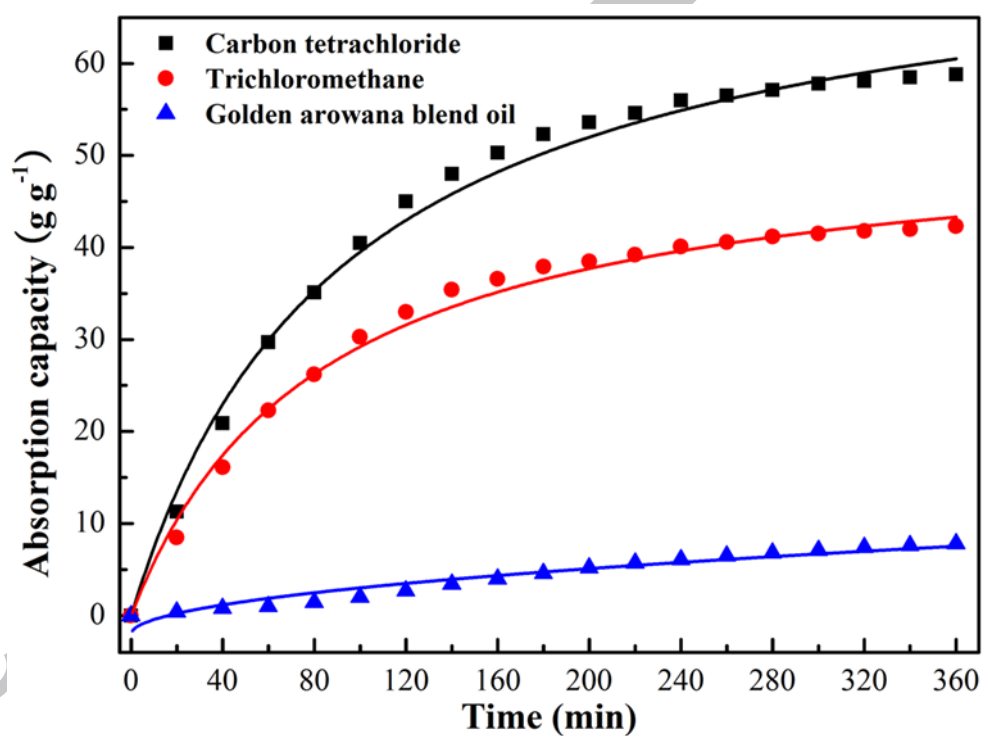


Figure 8. The time-dependent absorption capacity of carbon tetrachloride, trichloromethane and golden arowana blend oil on HCR-4; Black and red solid line were fitted from pseudo-second-order kinetic model, and blue solid line was fitted from intraparticle diffusion kinetic model.

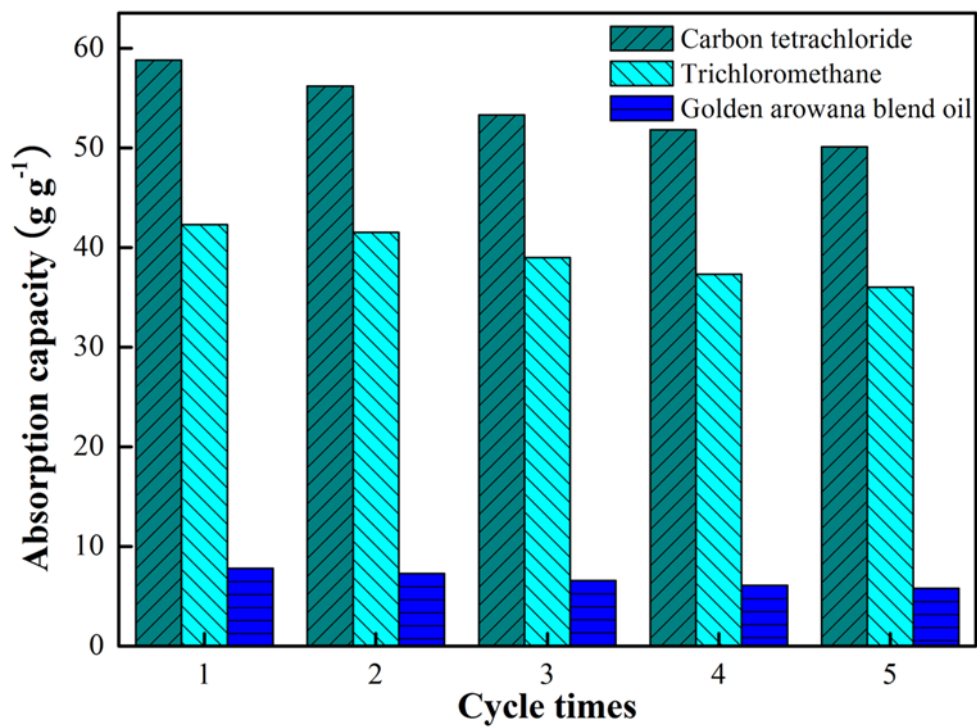


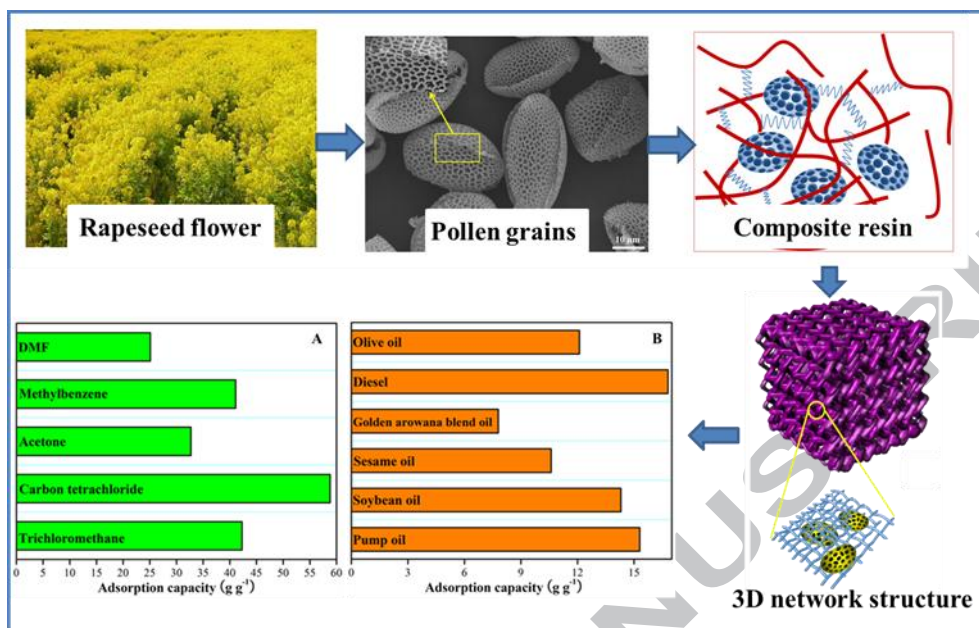
Figure 9. Recyclability and regeneration of HCR-4 for the absorption of Carbon tetrachloride, trichloromethane and golden arowana blend oil.

Table 1.

The values of parameters obtained by different kinetic models

Absorbates	Kinetics equations	R^2	q_e (g g ⁻¹)	q_{cal} (g g ⁻¹)	C
	$\ln(q_e - q_t) = \ln q_e - k_1 t$	0.979		72.9	
Carbon tetrachloride	$t/q_t = 1/(k_2 \cdot q_e^2) + t/q_e$	0.992	58.8	60.4	
	$q_t = k_3 t^{1/2} + C$	0.939		65.7	3.88
	$\ln(q_e - q_t) = \ln q_e - k_1 t$	0.987		47.9	
Trichloromethane	$t/q_t = 1/(k_2 \cdot q_e^2) + t/q_e$	0.993	42.3	43.3	
	$q_t = k_3 t^{1/2} + C$	0.930		47.3	3.70
	$\ln(q_e - q_t) = \ln q_e - k_1 t$	0.895		12.6	
Golden arowana	$t/q_t = 1/(k_2 \cdot q_e^2) + t/q_e$	0.319	7.80	-30.7	
blend oil	$q_t = k_3 t^{1/2} + C$	0.930		7.53	-2.27

Graphical abstract



Highlights

- Hydrophobic composite resin was synthesized via the introduction of pollen grains.
- The enhanced performance is due to well network structure and swelling properties.
- The absorption kinetics was employed to explore the absorption mechanism.
- The concept presented can be expanded to preparation of other composite resin.